

## Dielectric Anisotropy of a Homochiral Trinuclear Nickel(II) Complex

Da-Wei Fu,<sup>†</sup> Yu-Mei Song,<sup>‡</sup> Guo-Xi Wang,<sup>‡</sup> Qiong Ye,<sup>‡</sup> Ren-Gen Xiong,<sup>\*,†</sup> Tomoyuki Akutagawa,<sup>\*,‡</sup> Takayoshi Nakamura,<sup>‡</sup> Philip Wai Hong Chan,<sup>\*,§</sup> and Songping D. Huang<sup>\*,‡</sup>

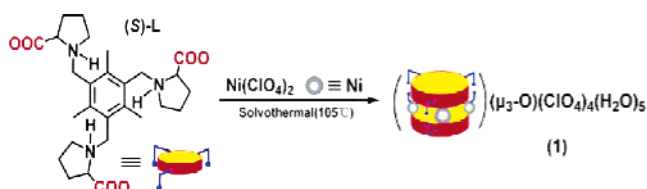
Ordered Matter Science Research Center, College of Chemistry and Chemical Engineering, Southeast University, Nanjing 210096, P. R. China, Research Institute for Electronic Science, Hokkaido University, Sapporo, 060-0812, Japan, Division of Chemistry and Biological Chemistry, School of Physical and Mathematical Sciences, Nanyang Technological University, Singapore 637616, Singapore, Department of Chemistry, Kent State University, Kent, Ohio 44242, and Nanjing University, Nanjing, P. R. China

Received January 10, 2007; E-mail: xiongrg@seu.edu.cn

Anisotropic properties have found widespread applications in many high technology fields such as polarized-lighted microscopy, quartz wedges useful for determining birefringence and optical sign, liquid crystals in large displays, thermal conductivity in microelectronic devices of solid-state transducers, nonlinear optical materials and single-molecule magnets, and pyroelectrics in infrared detectors.<sup>1</sup> Recently, artificial dielectric resonators with anisotropic character have also received much attention because of growing interest and needs of the electronics industry for such properties.<sup>2</sup> Most strong anisotropy on dielectric permittivity are known to only occur in the anomaly region with a phase transition and disappear beyond the phase-transition temperature range.<sup>3–5</sup> In this context, the development of continuous and stable large anisotropy on permittivity with temperature-independent property for practical applications such as solid transducers has remained relatively unexplored. We have performed measurements on anisotropic permittivity along three different directional crystallographic axes of homochiral trinuclear discrete Ni(II) complex (**1**) that was self-assembled by the hydrothermal reaction of Ni(ClO<sub>4</sub>)<sub>2</sub>·6H<sub>2</sub>O with TBPLA (Scheme 1).<sup>6</sup> Prior to this work, technologically useful properties such as second harmonic generation (SHG), ferroelectricity, and high dielectric permittivity behavior exhibited by homochiral complexes have been attributed to the fact that such complexes only crystallize in a noncentrosymmetric space group and the polar nature of the complex in the latter case. Herein, we report that **1** can exhibit a huge and stable and permanent dielectric anisotropy with temperature-independent feature with an increase of ca. 3.5 times of the ratio of  $\epsilon_r/c$  ( $E//c$ -axis)/ $\epsilon_r/b$  ( $E//b$ -axis) where  $\epsilon_r$  is the real part of the complex dielectric permittivity ( $\epsilon = \epsilon_r + i\epsilon_a$ ;  $\epsilon_a$  is the imaginary part). To our knowledge, a metal complex with such huge and permanent dielectric anisotropy that is temperature-independent is unprecedented.

A strong peak at 1113 cm<sup>-1</sup> in the IR spectrum of **1** indicates the presence of the perchlorate anion. A strong peak at 1673 cm<sup>-1</sup> that is associated with a strong peak at 1416 cm<sup>-1</sup> suggests the carboxylate group is deprotonated, which is confirmed by X-ray analysis (see later section). A second strong peak at 3426 cm<sup>-1</sup> indicates the presence of water. Thus, the TBPLA ligand is thought to be a zwitterionic neutral molecule similar to that of an amino acid and acts as a hexadentate chelator with each of the ligand's bidentate carboxylate moieties coordinated to the Ni atoms as shown in Figure 1. The molecular charge of **1** is balanced by four free ClO<sub>4</sub><sup>-</sup> anions and one  $\mu_3$ -O atom based on X-ray crystal structure

Scheme 1



analysis.<sup>7</sup> This results in the TBPLA ligand taking on a shape resembling that of a parachute, that is, exhibiting an all-cis coordination mode. Each Ni center displays a slightly distorted octahedron where its coordination geometry is composed of six O atoms in which four of the O atoms are from four different carboxylate groups, one O atom is from the oxo group and H<sub>2</sub>O. To our knowledge, this is the first example of a metal complex containing a homochiral C<sub>3</sub> symmetric ligand based on a literature search of the Cambridge X-ray crystallographic database. More notably, molecular packing analysis of **1** along each of the crystallographic axes reveals that the *c*-axis displays the largest molecular polarity while the polarity along the *b*-axis is the smallest (i.e.,  $P_s^{(001)} > P_s^{(100)} > P_s^{(010)}$  where  $P_s$  is the molecular polarity along the three axes, see Figures S1–S3 in the Supporting Information). This suggests that the anisotropic properties relative to molecular polarity should also display a same order. As anticipated, the Ni–O apical water bond distances are the longest among the Ni–O bond lengths and all of C–C, C–O, C–N, and Ni–O bond distances are comparable to literature values.

The temperature dependence of the ac dielectric permittivity measurements on an impedance analyzer on single crystals of **1** were carried out over the 5–300 K temperature range and a 10<sup>2</sup>–10<sup>6</sup> Hz frequency range. Electrical contacts were prepared using gold paste to attach the 10- $\mu$ m  $\phi$  gold wires to the single crystal. As shown in Figure 2, the permittivity  $\epsilon_r a$  of a single crystal of **1** along the *a*-axis ( $E//a$ , electric field approximately parallel to *a*-axis)

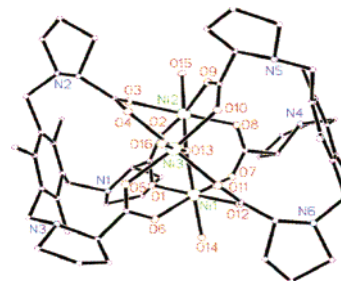


Figure 1. Asymmetric unit of **1** in which each Ni center displays distorted octahedron composed of four O atoms from four carboxylate groups and one O atom from water and another O atom from the oxo group. The crystallized water molecules, perchlorate anions, and H atoms are omitted for clarity.

<sup>†</sup> Southeast University.

<sup>‡</sup> Hokkaido University.

<sup>§</sup> Nanyang Technological University.

<sup>||</sup> Kent State University.

<sup>‡</sup> Nanjing University.

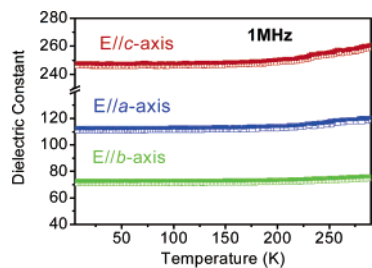


**Figure 2.** Dielectric permittivity ( $\epsilon_r$ ) of a single crystal of **1** as a function of temperature upon application of an electric field approximately parallel to the  $a$  ( $E//a$ ),  $b$  ( $E//b$ ), and  $c$  ( $E//c$ ) crystal axes directions. The measurements were made at a high frequency of 1 MHz.

reveals that the dielectric permittivity remains unchanged over the 5–300 K temperature range at a high frequency of 1 MHz and reaches a high value of  $\epsilon_r \approx 111$  with no frequency dependence observed over the  $10^{4.5}$ – $10^6$  Hz range (see Figure S4 in the Supporting Information). Similarly, the dielectric permittivity  $\epsilon_{rb}$  along the  $b$ -axis also remains constant with increasing temperature, reaching  $\epsilon_{rb} \approx 71$ . This allowed for the dielectric anisotropy of  $\epsilon_{ra}/\epsilon_{rb}$  to be estimated to be about 1.56. The temperature-independent dielectric behavior is similar to those found in metal-organic frameworks without guest where permittivity remains almost constant and the dielectric anisotropy is zero<sup>4</sup> and to nondeuterated organic solid acids in which permittivity also remains almost constant.<sup>8</sup> In addition, there is no frequency dependence of permittivity over the  $10^{4.5}$ – $10^6$  Hz range, or dielectric fluctuation is not large and negligible.

Surprisingly, the permittivity  $\epsilon_{rc}$  along the  $c$ -axis displays the largest value of  $\epsilon_{rc} \approx 246$  and dielectric behavior with increasing temperature and frequency comparable to those along the  $a$ - and  $b$ -axes. The dielectric anisotropy ratio of  $\epsilon_{rc}/\epsilon_{rb}$  and  $\epsilon_{rc}/\epsilon_{ra}$  are ca. 3.47 and 2.22, respectively. To our knowledge, such strong and stable dielectric anisotropy with temperature- and frequency-independence are unprecedented (see Supporting Information Figure S5 in which anisotropy remains constant basically) and can be qualitatively explained as follows. The relative dielectric permittivity should be proportional to the magnitude shown in

$$\begin{pmatrix} \epsilon_x & 0 & 0 \\ 0 & \epsilon_y & 0 \\ 0 & 0 & \epsilon_z \end{pmatrix} \begin{pmatrix} P_s^{(100)} \\ P_s^{(010)} \\ P_s^{(001)} \end{pmatrix} \quad (1)$$

When the electric field  $E$  is parallel to the  $c$ -axis [ $E//(001)$ ], the contribution from the  $a$ - and  $b$ -axes about the molecular polarity is negligible and  $\epsilon_x P_s^{(100)}$  and  $\epsilon_y P_s^{(010)}$  are also negligible. Thus, the dielectric magnitude along the  $c$ -axis is proportional to the product of  $\epsilon_z P_s^{(001)}$ . Since  $P_s^{(001)} > P_s^{(100)} > P_s^{(010)}$ , the product of  $\epsilon_z P_s^{(001)}$  is the largest when  $\epsilon_y P_s^{(010)}$  is the smallest, which is in good agreement with our dielectric experimental measurement results.

However, it should be noted that such huge dielectric anisotropy can be associated with strong ferroelectric property. To verify the ferroelectricity near room temperature, the hysteresis loop of electric polarization was measured on a single crystal or powdered sample of **1** approximately along the  $c$ -axis (Figure 3). This showed that the polarization ( $P$ )–electric field ( $E$ ) hysteresis curve to be typical of ferroelectrics; the spontaneous polarization ( $P_s$ ) reaches a relative high value of ca.  $3.4 \text{ nC/cm}^2$  at room temperature while the coercive field is relatively low, reaching ca.  $0.8 \text{ kV/cm}$  which is smaller than those typically found in ferroelectric polymers.<sup>3,9</sup>

The total macroscopic polarization should be parallel to the crystallographic  $c$ -axis, while the contribution from the  $a$ - and  $b$ -axis

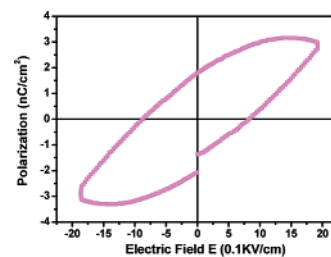


**Figure 3.** Hysteresis loops of electric polarization on a single crystal or powdered sample of **1** approximately parallel to the  $c$ -axis at room temperature. Ferroelectric magnitude was obtained by referring to the measured magnitude of KDP as standard value under the same measuring condition.

components of the two local dipoles in a unit cell should be ignored or be cancelled out by the 2-fold screw symmetry. This would account for the uniaxial spontaneous polarity and anisotropic behavior of the temperature-permittivity curves.

In summary, we have successfully performed anisotropic permittivity measurements on a novel homochiral trinuclear nickel(II) complex. For the first time, such a metal complex was shown to display huge and stable dielectric anisotropic effect with temperature-independent property. It is envisioned that our findings will provide new impetus for the development of new strategies to constructing high-technology devices.

**Acknowledgment.** This work was supported by 973 Project 2006CB806104, National Natural Science Foundation of China, EYTP of MOE (P. R. China), and a Start-up Grant from SEU. X.R.G. would like to thank the referees for their excellent suggestions. P.W.H.C. would like to thank NTU for funding.

**Supporting Information Available:** Detailed experimental procedures, IR' UV–vis, <sup>1</sup>HNMR, XPS, magnetic susceptibility, powdered dielectric permittivity, additional ORTEP views, and crystallographic cif file. This material is available free of charge via the Internet at <http://pubs.acs.org>.

## References

- (1) (a) Munir, A.; Hamanaga, N.; Kubo, H.; Awai, I. *Trans. Inst. Electron. Inf. Commun. Eng., Sect. E* **2005**, *E88-c*, 40. (b) Mironov, V. S.; Chibotaru, L. F.; Ceulemans, A. *J. Am. Chem. Soc.* **2003**, *125*, 9750. (c) Krebs, F. C.; Larsen, P. S.; Larsen, J.; Jacobsen, C. S.; Boutton, C.; Thorup, N. *J. Am. Chem. Soc.* **1997**, *119*, 1208.
- (2) (a) Lee, J.-S.; Kang, B. S.; Lin, Y.; Li, Y.; Jia, Q. X. *Appl. Phys. Lett.* **2004**, *85*, 2586. (b) Shumelyuk, A.; Barilov, D.; Odoulov, S.; Kratzig, E. *Appl. Phys.* **2003**, *B76*, 417.
- (3) (a) Horiuchi, S.; Kumai, R.; Tokura, Y. *J. Am. Chem. Soc.* **2005**, *127*, 5010. (b) Horiuchi, S.; Ishii, F.; Kumai, R.; Okimoto, Y.; Tachibana, H.; Nagaosa, N.; Tokura, Y. *Nat. Mater.* **2005**, *4*, 163. (c) Horiuchi, S.; Okimoto, Y.; Kumai, R.; Tokura, Y. *Science* **2003**, *299*, 229. (d) Horiuchi, S.; Kumai, R.; Okimoto, Y. *J. Am. Chem. Soc.* **1999**, *121*, 6757.
- (4) (a) Cui, H.-B.; Wang, Z.; Takahashi, K.; Okano, Y.; Kobayashi, H.; Kobayashi, A. *J. Am. Chem. Soc.* **2006**, *128*, 15074. (b) Cui, H.-B.; Takahashi, K.; Okano, Y.; Kobayashi, H.; Wang, Z.; Kobayashi, A. *Angew. Chem. Int. Ed.* **2005**, *44*, 6508.
- (5) (a) Katrusiak, A.; Szafranski, M. *J. Am. Chem. Soc.* **2005**, *127*, 15775. (b) Akutagawa, T.; Takeda, S.; Hasegawa, T.; Nakamura, T. *J. Am. Chem. Soc.* **2004**, *126*, 291.
- (6) TBPLA = (S)-1,1'-2,4,6-trimethylbenzene-1,3,5-triyl-tris(methylene)-tris-pyrrolidine-2-carboxylic acid.
- (7) Crystal data of **1**,  $C_{54}H_{86}Cl_4N_6Ni_3O_{34}$ ,  $M = 1681.22$ , monoclinic,  $P2_1$ ,  $a = 13.554(5) \text{ \AA}$ ,  $b = 12.809(5) \text{ \AA}$ ,  $c = 22.151(8) \text{ \AA}$ ,  $\beta = 99.081(5)^\circ$ ,  $V = 3798(2) \text{ \AA}^3$ ,  $Z = 2$ ,  $D_c = 1.470 \text{ Mg m}^{-3}$ ,  $R_1 = 0.0643$ ,  $wR_2 = 0.1364$ ,  $\mu = 0.965 \text{ mm}^{-1}$ ,  $S = 1.033$ ; Flack = 0.042(17).
- (8) (a) Takasu, I.; Izuka, A.; Sugawara, T.; Mochida, T. *J. Phys. Chem. B* **2004**, *108*, 5527. (b) Moritomo, Y.; Tokura, Y.; Takahashi, H.; Mori, N. *Phys. Rev. Lett.* **1991**, *67*, 2041.
- (9) (a) Ye, Q.; Song, Y.-M.; Wang, G.-X.; Fu, D.-W.; Chen, K.; Chan, P. W. H.; Zhu, J.-S.; Huang, D. S.; Xiong, R.-G. *J. Am. Chem. Soc.* **2006**, *128*, 6554. (b) Okubo, T.; Kawajiri, R.; Mitani, T.; Shimoda, T. *J. Am. Chem. Soc.* **2005**, *127*, 17598.

JA0701816